

# Investigation on O<sub>3</sub> and NO<sub>x</sub> Production in a Surface DBD

C. Piferi<sup>1</sup>, G. Pierotti<sup>2</sup>, M. Cavedon<sup>1</sup>, A. Popoli<sup>2</sup>, E. Martines<sup>1</sup>, A. Cristofolini<sup>2</sup>, C. Riccardi<sup>1</sup>

<sup>1</sup> *Dipartimento di Fisica "Giuseppe Occhialini", University of Milano-Bicocca, Piazza della Scienza 3, 20126 Milano, Italy*

<sup>2</sup> *Department of Electrical, Electronic and Information Engineering "Guglielmo Marconi", University of Bologna, Viale Risorgimento 2, 40136 Bologna, Italy*

**Introduction** Dielectric Barrier Discharges (DBD) have been used for a very long time for different applications, such as ozone generators, excimer lamps, plasma discharge panels, air and surface modifications [1,2]. These devices are characterized by the presence of an insulating material between the electrodes to prevent the generation of high electrical current arcs between them [3]. The plasma produced is non-thermal at atmospheric pressure in the discharge gap region between electrodes [4,5]. If the gap between the electrodes is reduced to zero, the region where the plasma can be generated is over the dielectric surface. These devices are usually called Surface Dielectric Barrier Discharges (SDBD) [6].

The purpose of this work is the development of an experimental setup able to detect the O<sub>3</sub> and NO<sub>x</sub> species produced by an SDBD discharge using absorption spectroscopy.

A 0D kinetic model has been implemented to study the time-evolution of the main neutral species produced by the discharge. The model is based on a simplified set of reactions for synthetic dry air at atmospheric pressure. The results yielded by the 0D numerical model are compared to the experimental measurements.

**Experimental setup** We placed (Fig. 1) an SDBD device inside a vacuum box sealed at two opposite sides by quartz windows and at the other two ends by open-close valves. In front of one of the quartz windows we placed the lamps, while at the other side the radiometric detectors [7]. As we are also interested in measuring the temperature, one temperature probe was placed in contact with the ground side of the SDBD (contact temperature), while a second one was placed in the chamber (air temperature). Finally, to insure uniformity of the gas, a fan has been placed inside the chamber. For every experiments,

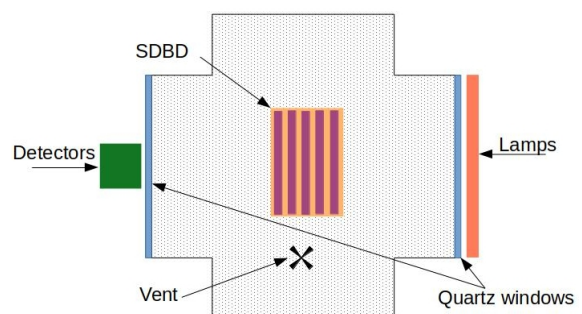


Figure 1: *Scheme of the experimental setup.*

we filled the box with pure air and we close the valves before lighting the plasma.

Absorption spectroscopy is used to determine the reactive species densities  $n$ . We estimated the species' production according to the Lambert-Beer law:  $n = -\frac{\log\left(\frac{I}{I_{\text{no plasma}}}\right)}{Lc}$  where  $I$  is the intensity when the plasma is on,  $I_{\text{no plasma}}$  is the intensity when the plasma is off,  $L$  is the distance between the lamps and the probe, and  $c$  is the absorption coefficient.

**Experimental results** We measured  $\text{O}_3$  and  $\text{NO}_2$  concentrations as well as the contact and air temperature for different power levels (Fig. 2). Note that in Fig. 2 (a) and (b), which are at low input power, are plotted on a time scale from 0 to 600 s, while (c) and (d), that are at high input power, are from 0 to 220 s.

Different  $\text{O}_3$  regimes are identified at different input powers. The slope at the ignition is steeper for increasing power levels. The maximum  $\text{O}_3$  number density decreases with the input power. Also, the decrease happens at lower treatment times for higher power levels. For low input power, we reach an instrumental saturation due to the high  $\text{O}_3$  concentration that absorbs all the light emitted by the sources. This saturation corresponds to  $4 \times 10^{16} \text{ cm}^{-3}$ , meaning that we are not able to detect the real peaks for the  $\text{O}_3$  produced by plasma at 12 W of input power.

For high power, the nitrogen oxidation chain is responsible for the  $\text{O}_3$  depletion and the  $\text{NO}_2$  fast increase.

The maximum contact temperature it is strictly dependent on the power, while the air temperature slightly increases from the initial value and stabilizes in a short time.

### Numerical model and comparison

The model is based on the plasma-chemistry set of reactions proposed in [8], consisting of 36 processes and five fitting parameters. these latter are the number densities of O,  $\text{O}_2(\text{a})$ ,  $\text{N}_2(\text{A})$ , the  $\text{N}_2$  steady-state vibrational temperature and the time constant of the vibrational temperature increase. The vibrational temperature regulates the number density of the vibrationally excited nitrogen molecules. Assuming a Maxwellian distribution of the vibrational energy, the following relation can be written:  $n_{\text{N}_2(\text{v})} = n_{\text{N}_2} \exp\left(-\frac{12\Delta\varepsilon_{\text{v}}}{k_{\text{B}}T_{\text{v}}}\right)$  where  $n_{\text{N}_2(\text{v})}$  is the number density of the nitrogen vibrational state above level 12,  $n_{\text{N}_2}$  is the number density of the ground state nitrogen molecules,  $k_{\text{B}}$  is the Boltzmann constant,  $T_{\text{v}}$  is the vibrational temperature and  $\Delta\varepsilon_{\text{v}}$  is the vibrational energy for a harmonic oscillator. The described kinetic scheme has been implemented in Fortran language, using the ZDPlaskin module [9]. The results yielded by the performed numerical simulation are compared to the experimental data in Fig. 3. The numerical results are in good agreement with the experimental data. Note that the rate coefficients for reaction 5

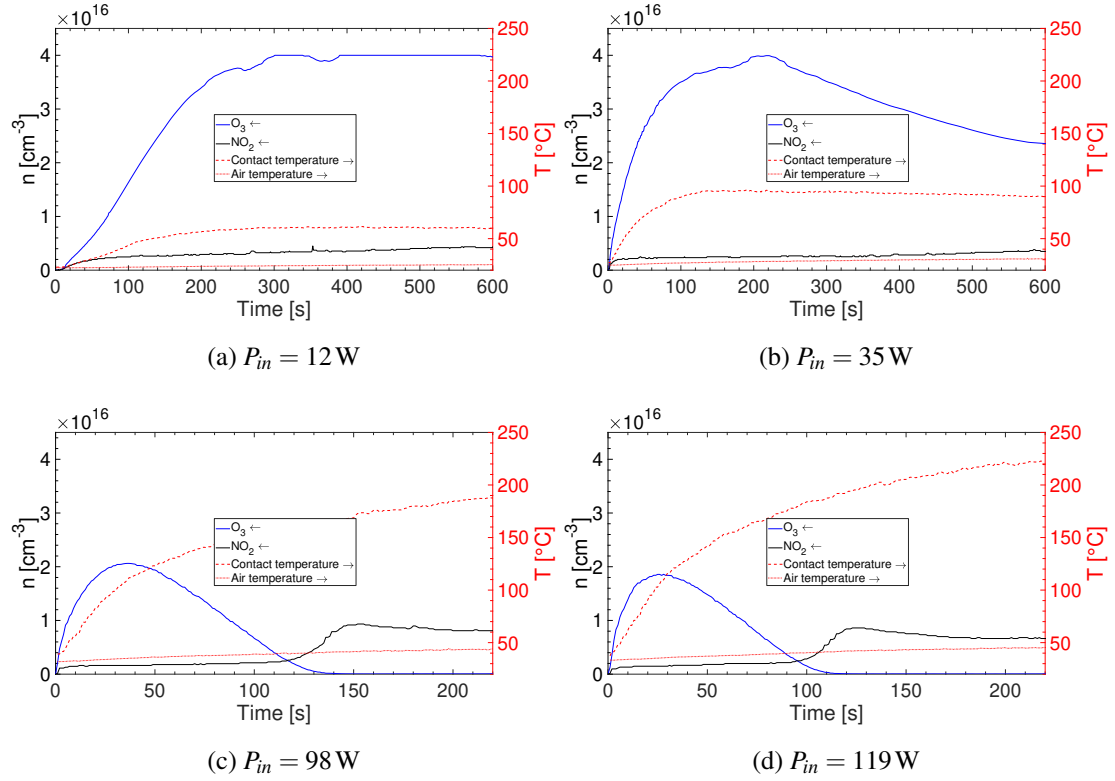


Figure 2: (left axis) Density of  $O_3$  and  $NO_2$  and (right axis) contact and ambient temperature for different input power levels: (a)  $P_{in} = 12$  W, (b)  $P_{in} = 35$  W, (c)  $P_{in} = 98$  W (d)  $P_{in} = 119$  W.

reported in [8] ( $O + NO \longrightarrow NO_2$ ) is not consistent with the one found in [10]. The latter is used in our simulations.

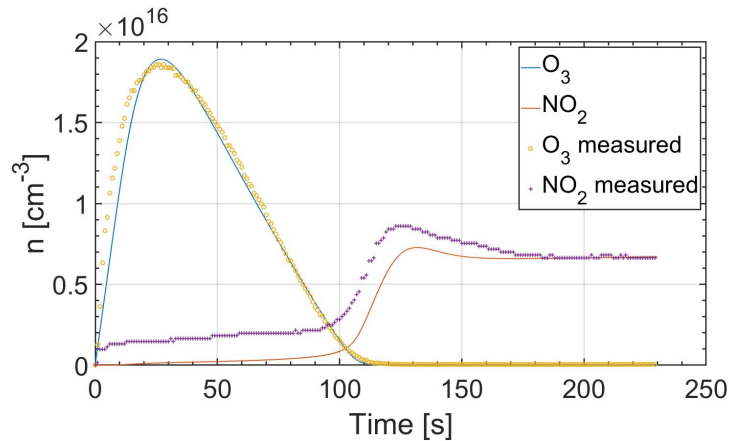


Figure 3: Comparison between experimental data and numerical results for  $P_{in} = 119$  W

Future scientific efforts will be focused on developing and implementing a more detailed plasma chemistry model, to be used in place of the one described in this work. The detailed model will feature an expanded set of reactions and will be composed of two coupled sub-

models, a *discharge* one and an *afterglow* one. The first sub-model aims is to assess the production rate of some key species (atomic oxygen, molecular oxygen and molecular nitrogen excited levels), due to the discharge. The second sub-model is devoted to the afterglow region instead. The results obtained using this approach are currently under validation.

## References

- [1] A. Cristofolini, A. Popoli, and G. Neretti, International Journal of Applied Electromagnetics and Mechanics **63**, S1, (2020)
- [2] S. Zanini, E. Grimoldi, A. Citterio, C. Riccardi, Applied Surface Science **349**, (2015)
- [3] C. Piferi, R. Barni, H. E. Roman, C. Riccardi, Applied Sciences **11**, 5 (2021)
- [4] I. Biganzoli, R. Barni, C. Riccardi, Review of Scientific Instruments **84**, 1 (2013)
- [5] I. Biganzoli, R. Barni, A. Gurioli, R. Pertile, C. Riccardi, Journal of Physics: Conference Series **550**, (2014)
- [6] G. Colonna, C. D. Pintassilgo, F. Pegoraro, A. Cristofolini, A. Popoli, G. Neretti, A. Gicquel, O. Duigou, T. Bieber, K. Hassouni and L. Laguardia European Physical Journal D **75**, 6 (2021)
- [7] C. Piferi, A. Brescia, C. Riccardi, AIP Advances **11**, 8 (2021)
- [8] S. Park, W. Choe, and C. Jo, Chemical Engineering Journal **352**, (2018)
- [9] S. Pancheshnyi, B. Eismann, G. J. M. Hagelaar, and L. C. Pitchford, Computer code ZDPlasKin (2018). University of Toulouse, LAPLACE, CNRS-UPS-INP, Toulouse, France.
- [10] M. Capitelli, C. M. Ferreira, B. F. Gordiets, and A. I. Osipov, Springer Science and Business Media (2013).